Analysis of the Effects of Phase Noise in Filtered Multitone (FMT) Modulated Systems

Antonio Assalini, Silvano Pupolin
Dept. of Information Engineering – DEI
Padova, Italy
e–mail: {assa, pupolin}@dei.unipd.it

Andrea M. Tonello
Dept. of Electrical Engineering – DIEGM
Udine, Italy
e–mail: tonello@diegm.uniud.it

***Abstract*— In this paper, we study the effects of phase noise in a multicarrier system. We show that the phase noise introduces interference components, and we evaluate their second order statistics. The analysis is then applied to two particular multicarrier architectures: discrete multitone (DMT) modulation, and filtered multitone (FMT) modulation. For the DMT case our results are in agreement with other related work that considers DMT only. For FMT modulation we demonstrate that the phase noise power spectral density as well as the frequency response of the prototype filters play a key role on the resulting interference power value. Finally, we show that the analytical performance results are close to the simulation results.**

I. Introduction

Multicarrier based transmission is an effective signaling technique that allows to achieve high spectral efficiencies over wideband channels with possibly lower complexity than single carrier modulation. Discrete multitone (DMT) modulation, that is usually referred to as orthogonal frequency division multiplexing (OFDM), has been deployed in many communication systems, e.g. IEEE 802.11a/g, IEEE 802.16a, DVB-T, UMTS, ADSL, and HomePlug. In this paper, we also consider another multicarrier architecture that is known as filtered multitone (FMT) modulation. FMT has been proposed for very high-speed digital subscriber line (VDSL) [1] and its application to wireless transmission is under investigation [2]-[7].

It has been shown that DMT is more sensible than single carrier transmission to the phase noise that is introduced by the oscillators in the receiver front-end [8]–[11]. This translates in more stringent tuner requirements and consequently in higher costs. Preliminary results have shown that also FMT is sensible to the phase noise [5]. In this paper we carry out a detailed analysis of the effects of phase noise in an FMT modulated system.

After the system description of Sec.I, we describe in Sec.II the various effects that the phase noise generates in a general multicarrier system. We evaluate the power of the interfering component in Sec.III. In Sec.V we particularize the analysis to DMT and FMT considering the phase noise model that is described in Sec.IV. Simulation results and theoretical performance bounds are compared in Sec.VI.

§This work was supported in part by the Italian Ministry of Education, University and Research under the FIRB project: "Reconfigurable platforms for wideband wireless communications", prot. RBNE018RFY.

II. Transmission System Description

In Fig.1 we depict a general multicarrier system with M subcarriers that assumes a discrete-time implementation [1][2]. The information data sequences $a_m(nT), m = 0, 1, ..., M-1$, are up-sampled and shaped with a filter centered on a given subcarrier. The resulting modulated signal is the sum of M contributions. We assume the data symbols to be independent and identically distributed (i.i.d.) with zero-mean and power M_{a_m}. The sub-channel shaping pulse $h(t)$ is identical for all sub-channels and is referred to as prototype filter. This scheme collapses in a discrete multitone (DMT) or in a filtered multitone (FMT) scheme depending on the choice of $h(t)$ and of the up–sampling factor K. In particular, if $h(t)$ has time-limited rectangular impulse response and $K = M$, we obtain the well known DMT (commonly named OFDM) solution. Otherwise, if $h(t)$ is designed for obtaining an ideal frequency separation between adjacent sub-channels, the modulator is called FMT. We have a critically sampled (CS-FMT) or non–critically sampled (NCS-FMT) solution if $K = M$ or $K > M$, respectively. The transmission bandwidth $B_s = 1/T_c = K/T$ is then subdivided in M equally spaced subchannels with frequency separation given by $B = B_s/M$. At the receiver side, after down-conversion and analog-to-digital conversion, the dual base-band operations are implemented using a prototype filter $g(t)$ matched with $h(t)$. Both the DMT and the FMT modulator/demodulator can be efficiently implemented via a fast Fourier transform (FFT) [1].

In the following sections, we carry out an in-depth analysis of the effects of phase noise into these modulation systems. As shown in Fig.1, phase noise can be modelled as a multiplicative factor, $\exp\{\phi(t)\}$, that randomly varies the phase of the received signal. $\phi(t)$ is a stationary random process with zero mean and a given power spectral density (PSD). We remark that usually the transmission chain includes the digital-to-analog and the analog-to-digital converters whose effect is to limit the bandwidth of the modulated signal and of the phase noise PSD.

Proc. of IEEE Globecom 2004, Dallas, Nov. 29 - Dec. 3, 2004, pp. 3541-3545

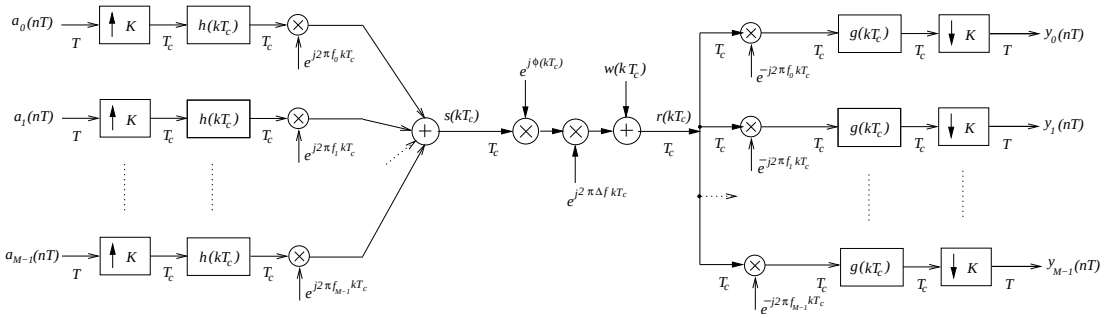

Fig. 1. Multicarrier modulation/demodulation chain impaired by phase noise and frequency offset.

III. Phase Noise Effects

In the sequel we analyze the effects of phase noise in a general multicarrier system as described by Fig.1. In the successive sections the effects will be particularized for the DMT and the FMT solutions.

The modulated signal $s(kT_c)$ can be written as[1],

$$s(kT_c) = \sum_{i=0}^{M-1} e^{j2\pi f_i kT_c} \sum_{n=-\infty}^{+\infty} a_i(nT)\, h(kT_c - nT)\,. \quad (1)$$

Assuming transmission through an additive white Gaussian noise (AWGN) channel, the received base-band signal is corrupted by the additive thermal noise $w(kT_c)$ and distorted by the time varying phase noise $\phi(kT_c)$[2]:

$$r(kT_c) = s(kT_c)\, e^{j\phi(kT_c)} + w(kT_c)\,. \quad (2)$$

The real and imaginary components of the i.i.d. AWGN samples have variance $\sigma_w^2 = N_0/2$.

Focusing the analysis on the l-th subchannel, $l = 0, 1, .., M-1$, the matched filter output sample reads

$$\begin{aligned} y_l(nT) &= \sum_{k=-\infty}^{+\infty} r(kT_c)\, e^{-j2\pi f_l kT_c} g(nT - kT_c) \\ &= a_l(nT)\, z_{l,l}(nT, nT) + \sum_{\substack{p=-\infty \\ p\neq n}}^{+\infty} a_l(pT)\, z_{l,l}(pT, nT) \\ &\quad + \sum_{\substack{i=0 \\ i\neq l}}^{M-1} \sum_{p=-\infty}^{+\infty} a_i(pT)\, z_{i,l}(pT, nT) + w'(nT) \end{aligned} \quad (3)$$

where we have defined

$$\begin{aligned} z_{i,l}(pT, nT) = \sum_{k=-\infty}^{+\infty} & e^{j\phi(kT_c)} e^{j2\pi(f_i - f_l)kT_c} \\ & \times h(kT_c - pT)\, g(nT - kT_c)\,. \end{aligned} \quad (4)$$

[1]*Notation.* Lower (capital) cases letters represent the signal in the time (frequency) domain. The convolution operator is indicated as $\circledast$. $E[.]$ is the expectation operator. $\mathrm{r}_\psi(t)$ and $\mathrm{R}_\psi(f)$ are the autocorrelation and the PSD of the random process ψ, respectively. The Kroenecher operator is $\delta(\cdot)$.

[2]We have assumed that the phase noise $\phi(t)$ is constant over a period T_c, this is a common approximation that holds true when the phase-noise is slowly varying with respect to T_c. In general ([12]), when an integrate-and-dump filter is used at the receiver, the term $\exp\{j\phi(kT_c\}$ is replaced by $\frac{1}{Tc}\int_{(k-1)T_c}^{kT_c} \exp(j\phi(t))dt$.

The sequence of filtered noise samples $w'(nT)$ is a stationary Gaussian random process with zero mean, variance $\sigma_{w'}^2$, and PSD $R_{w'}(f) = N_0\,|G(f)|^2$.

Now, looking at (3) we find out that three different interference contributions exist in the presence of phase noise. The prototype filters play a key role for the characterization of such interfering components. Therefore, different effects are expected for DMT and FMT as we show in Section VI.

The first term in (3) contains the transmitted information symbol, that is randomly rotated and attenuated by a common phase error (CPE) $z_{l,l}(nT, nT)$ [8], [10]. The second term corresponds to the intersymbol interference (ISI) due to the symbols transmitted on the same subchannel. Finally, the last contribution is the interference generated by the symbols transmitted over other subchannels. The carrier interference (CI) can be separated in the *Intra*–CI due to the symbols transmitted at the same time of the useful one, and in the *Inter*–CI due to the symbols transmitted at other time instants.

IV. Analysis of the Interfering Components

In this section we report an analysis of the interfering components, i.e. CPE, ISI, Intra/Inter-CI.

A. Evaluation of the Mean of the Interference Components

Assuming $h(t)$ perfectly matched with $g(t)$, it can be shown that the ISI and the Intra/Inter–CI contributions have zero mean. Instead, the mean of the CPE is given by

$$\begin{aligned} \bar{\theta}_{\mathrm{CPE},l} &= E[z_{l,l}(nT, nT)] \\ &= E[e^{j\phi(kT_c)}] \sum_{k=-\infty}^{+\infty} h(kT_c - nT)\, g(nT - kT_c)\,. \end{aligned} \quad (5)$$

We observe that the CPE is subcarrier independent, i.e. all transmitted symbols exhibit the same common phase error, such that $\bar{\theta}_{\mathrm{CPE},l} = \bar{\theta}_{\mathrm{CPE}}$, $l = 0, 1, ..., M-1$.

It is useful to define the common phase interference (CPI) as the varying part of the CPE [8], i.e. $\tilde{z}_{l,l}(nT, nT) = z_{l,l}(nT, nT) - \bar{\theta}_{\mathrm{CPE}}$. CPI is a random variable with zero mean.

B. CPI, ISI and Intra/Inter–CI Power Evaluation

The statical power of the interfering components can be evaluated exploiting the filter shape and the PSD of the phase noise. The analysis in this section assumes no correction of any phase errors, i.e. a *non–coherent receiver*.

Let us define the first factor that appears in the sum in (4) as

$$\begin{aligned}\vartheta_{i,l}(kT_c) &= e^{j\phi(kT_c)} e^{j2\pi(f_i - f_l)kT_c} \\ &= \theta(kT_c)\, e^{j2\pi(f_i - f_l)kT_c}\,.\end{aligned} \tag{6}$$

It is simple to show that its PSD is given by

$$\mathrm{R}_{\vartheta_{i,l}}(f) = \mathrm{R}_{\theta}(f - (f_i - f_l))\,. \tag{7}$$

Equation (4) can be rewritten as a 2-dimensional convolution (the filters are real and even):

$$\begin{aligned}z_{i,l}(t_1,t_2) &= \sum_k \sum_p s_{i,l}(kT_c, pT_c)\, q(t_1 - kT_c, t_2 - pT_c) \\ &= s_{i,l} \circledast q(t_1,t_2)\,, \qquad t_1, t_2 \in \{..., -2T, -T, 0, T, 2T...\}\end{aligned} \tag{8}$$

where $s_{i,l}(kT_c, pT_c) = \vartheta_{i,l}(kT_c)\delta(pT_c - kT_c)$ is function of the phase noise samples and $q(t_1,t_2) = h(t_1)\, g(t_2)$ is the impulse response of a 2-dimensional filter. Eq. (8) represents a 2-dimensional up-sampling and filtering operation.

To proceed with the analysis, it is useful to compute the bi-dimensional PSD of the non-stationary random process $z_{i,l}(t_1,t_2)$ in (8). The computation yields

$$\mathrm{R}_{z_{i,l}}(f_1,f_2) = \mathrm{R}_{\vartheta_{i,l}}(f_1 + f_2)\, |Q(f_1,f_2)|^2\,. \tag{9}$$

We observe that the frequency response of the filter $q(t_1,t_2)$ is separable: $Q(f_1,f_2) = H(f_1)\, G(f_2)$. The statical power of the interfering components can be calculated exploiting (9) (see Appendix I). The Intra/Inter-CI has zero mean, and its variance can be calculated as

$$\sigma^2_{\mathrm{CI},l} = \sum_{i=0, i\neq l}^{M-1} M_{a_i} \int_{-B_s/2}^{+B_s/2} \mathrm{R}_{\vartheta_{i,l}}(f)\; |G(f)|^2\, |H(0)|^2\, df\,, \tag{10}$$

where M_{a_i} is the power of the information symbols transmitted over the i-th subchannel. The power of the CPE plus ISI becomes:

$$M_{\mathrm{CPE+ISI},l} = M_{a_l} \int_{-B_s/2}^{+B_s/2} \mathrm{R}_{\vartheta_{l,l}}(f)\; |G(f)|^2\, |H(0)|^2\, df\,. \tag{11}$$

Remembering that the mean of this interference contribution is $\bar{\theta}_{\mathrm{CPE}}$, the interfering variance can be calculated as:

$$\sigma^2_{\mathrm{CPI+ISI},l} = M_{\mathrm{CPE+ISI},l} - M_{a_l} |\bar{\theta}_{\mathrm{CPE}}|^2\,. \tag{12}$$

Finally, the average signal–to–noise plus interference ratio on the l–th subcarrier $SNIR_l$ can be obtained as

$$SNIR_l = \frac{M_{a_l} \bar{\theta}^2_{\mathrm{CPE}}}{\sigma^2_{\mathrm{CI},l} + \sigma^2_{\mathrm{CPI+ISI}\ ,l} + \sigma^2_{w'}}\,. \tag{13}$$

C. Including a frequency offset

The effects of a constant frequency offset can be easily included in the proposed analysis. Let Δf the carrier frequency offset (CFO) between the transmitted and the received signal, Fig.1. The joint effects of CFO and phase noise can be evaluated using: $\mathrm{R}_{\vartheta_{i,l}}(f) = \mathrm{R}_{\theta}(f - (f_i - f_l + \Delta f))$, instead of (7). As shown in [4], CFO introduces both ISI and Intra/Inter–CI into the modulated signal.

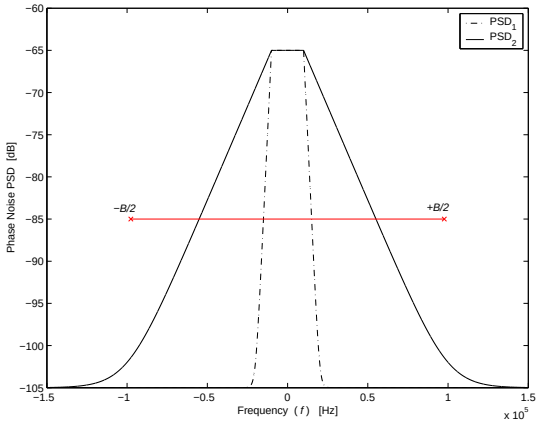

Fig. 2. PSDs of the phase noise given in (14), with $a = 6.5$, $b = 4$, and $c = 10.5$. The PSD_1 has $f_{\phi_1} = 10K$Hz and $f_{\phi_2} = 20K$Hz, while for PSD_2, $f_{\phi_1} = 10K$Hz and $f_{\phi_2} = 100K$Hz

V. Phase Noise Model

In literature there are different proposed models for the phase noise [8]–[12]. As an example we report a model of phase noise $\phi(t)$ with finite power described by the following PSD function:

$$\mathrm{R}_{\phi}(f) = 10^{-c_\phi} + \begin{cases} 10^{-a_\phi}, & |f| \le f_{\phi_1} \\ 10^{-(|f| - f_{\phi_1})\frac{b_\phi}{f_{\phi_2} - f_{\phi_1}} - a_\phi}, & |f| > f_{\phi_1} \end{cases} \tag{14}$$

The coefficient c_ϕ determines the noise floor, b_ϕ the steepness of the slope, a_ϕ and f_{ϕ_1} establish the white phase noise region and f_{ϕ_2} is the frequency where the noise-floor is dominant [10]. In Fig. 2 the PSD is reported for two different values of f_{ϕ_1} and f_{ϕ_2}.

If we assume the standard deviation of the phase noise small enough, i.e. $\sigma_\phi << 1$, the term $\theta(t)$ in (6) can be rewritten using a series expansion:

$$\theta(t) = e^{j\phi(t)} \simeq 1 + j\phi(t) - \phi(t)^2/2\,. \tag{15}$$

In this case, the PSD of $\theta(t)$ is well approximated by:

$$\mathrm{R}_{\theta}(f) = \delta(f) + \mathrm{R}_{\phi}(f)\,. \tag{16}$$

VI. Phase Noise Effects in DMT and FMT systems: Limits for a Non–Coherent Receiver

In the DMT system the modulator and demodulator constituent filters have time–limited impulse responses given by

$$h(kT_c) = g(kT_c) = \begin{cases} 1, & \text{if } \ 0 \le k \le M-1 \\ 0, & \text{otherwise} \end{cases}\,. \tag{17}$$

In a FMT system the prototype filter has a frequency-limited shape. Ideally the filters have rectangular frequency response:

$$H(f) = \begin{cases} 1, & \text{if } \ |f| \le 1/2T = B_s/2K = B/2 \\ 0, & \text{otherwise} \end{cases}\,. \tag{18}$$

At the receiver side $g(t)$ is matched with $h(t)$, $g(t) = h^*(-t)$.

Firstly, since $\phi(t)$ is a zero mean random variable, the mean of the CPE (5) is $\bar{\theta}_{CPE} = 1 - P_\phi/2$, where (15) has been used and $P_\phi = \sigma^2_\phi$. The $\bar{\theta}_{CPE}$ is equal in both DMT and FMT systems.

A. DMT

In the DMT system, the ISI and Inter–CI components disappear (Eq. (8), and [11]). The power of the CPE plus Intra-CI becomes:

$$M_{\text{CPE+Intra-CI},l} = \sum_{i=0}^{M-1} M_{a_i} \int_{-B_s/2}^{+B_s/2} \mathrm{R}_{\vartheta_{i,l}}(f)\ \mathrm{sinc}^2(fT)\, df\,. \tag{19}$$

This result is in agreement with [10]. In [8] it has been shown that if $|\phi(t)| \ll 1$, than the total power of the interfering signals is only function of P_ϕ, i.e. $\sigma^2_{\text{Inttra-CI+CPI},l}|_{\text{DMT}} = M_a P_\phi$, with $M_{a_i} = M_a$, $\forall i$. However, we remark that the individual contributions of CPI and Intra-CI are a function of the phase noise PSD shape.

B. CS/NCS–FMT

In an FMT based system the evaluation of the effects of the phase noise can be effectively evaluated with the proposed method. Using the ideal filter in (18), the power of the CPE plus ISI is

$$M_{\text{CPE+ISI},l} = M_{a_l} \int_{-B/2}^{+B/2} \mathrm{R}_{\vartheta_{l,l}}(f)\, df\,. \tag{20}$$

We conclude that the auto–interference on subcarrier l is a function of the phase noise shape. In particular it depends on the amount of phase noise power that falls in the l-th sub-channel. Moreover, we observe that NCS–FMT is less sensible than CS–FMT, this is because the prototype filter bandwidth in NCS–FMT is smaller than in CS–FMT, i.e. $B_s/K < B_s/M$ (B_s is fixed) [1][3][4]. Similar observations are possible for the Intra/Inter–CI power evaluation (see (10)). However for a CS-FMT modulator, when $M_{a_i} = M_a$, $\forall i$, the global interfering contribution has power:

$$\sigma^2_{\text{CPI+ISI+CI},l}|_{\text{CS-FMT}} = M_a P'_\phi\,, \tag{21}$$

where P'_ϕ is the amount of phase noise power that falls in the signal bandwidth B_s. In general this inequality holds:

$$\sigma^2_{\text{CPI+ISI+CI},l}|_{\text{NCS-FMT}} \leq \sigma^2_{\text{CPI+ISI+CI},l}|_{\text{CS-FMT}}\,. \tag{22}$$

Briefly, for a fixed signal bandwidth B_s the sensitivity to the phase noise can change as function of the FMT parameters as follows (under the assumption of an ideal prototype filter):

(i) In CS-FMT, the global power of the interference doesn't depend on the number of subcarriers M, but only by the phase noise power that falls in the bandwidth B_s.

(ii) In NCS-FMT, performance is function of the up–sampling factor K. The performance degradation decreases if K increases (but the spectral efficiency is also reduced). Fixing K, the system is more sensitive to the phase noise for a lower number of subcarriers. The phase noise spectra shape plays a key role.

(iii) Fixing the power of the phase noise that falls in B_s, the PSD $\mathrm{R}_\phi(f)$ determines the distribution of the interference power between the CPI plus ISI and the Intra/Inter–CI.

The prototype filter shape influences the phase noise effects. Usually, the filters are designed to achieve robustness to ISI and Intra–CI [2]. Note that the analysis in Sec.IV includes the effects of residual interference due to a non–ideal shape of the prototype filter. We show in Fig.3 the power of the interference on a particular subchannel for DMT, CS-FMT, and NCS-FMT. The FMT systems use an ideal rectangular in frequency prototype pulse. We note that in the FMT systems the Intra/Inter–CI is negligible with respect to the CPI and ISI components. Moreover, we observe that in a DMT system, the Inter–CI is evident. We remark that we have evaluated the interference power for each subchannel right after the matched filter-bank. Usually, in a FMT modulated system, equalization is necessary with the purpose of reducing the ISI caused by the prototype filter and multipath radio channel [1], [7]. However, in the simulation results of the next section, performance is evaluated considering also equalization.

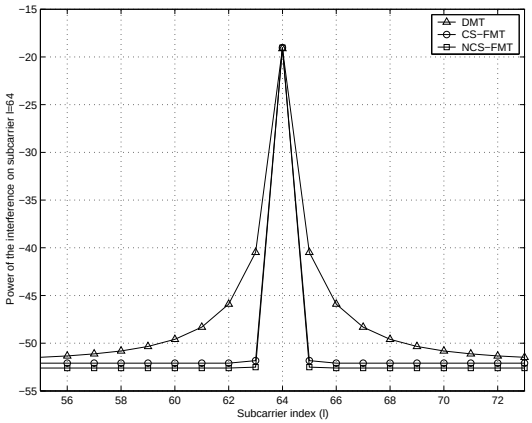

Fig. 3. Power of the interfering component on the subcarrier $l = 64$ ($M = 128$). The PSD_2 of Fig. 2 is used for the phase noise modelling.

VII. Simulation Results

We consider DMT and FMT modulated systems with $M = 128$ subcarriers over a frequency band of $B_s = 25M$Hz. The FMT prototype filter $h(t)$ that we choose, has temporal extension $t \in \{0, T_c, ..., (\gamma - 1)T_c\}$, with $\gamma = 12$. In the NCS–FMT scheme the prototype filter approximates a square–root raised cosine pulse with a roll–off $\rho = 0.125$. The up–sampling factor is $K = (1 + \rho)M = 144$. For the correction of the residual ISI due to the FMT prototype filter we use a per-subcarrier fractionally–spaced ($T/2$) decision feedback equalizer (FS–DFE) with 12 coefficients for both the feedforward and the feedback filters.

In Fig.4 the bit error rate (BER) versus the signal–to–noise ratio SNR (defined as $SNR = E[|s(kT_c)|^2]/(N_0 B_s/M)$) is shown for both DMT and NCS-FMT in the presence of phase noise over an AWGN channel. Both QPSK and 16-QAM mapping are considered for the two phase noise PSDs of Fig.2. The figures show that the performance degradation increases with the modulation order in both DMT and FMT.

Moreover, we report also the theoretical performance that is computed by using the $SNIR$ defined in (13). The theoretical bounds are close to the simulated performance. We emphasize that in NCS-FMT with the employed prototype filter and with the considered phase noise PSDs, the Intra/Inter-CI is

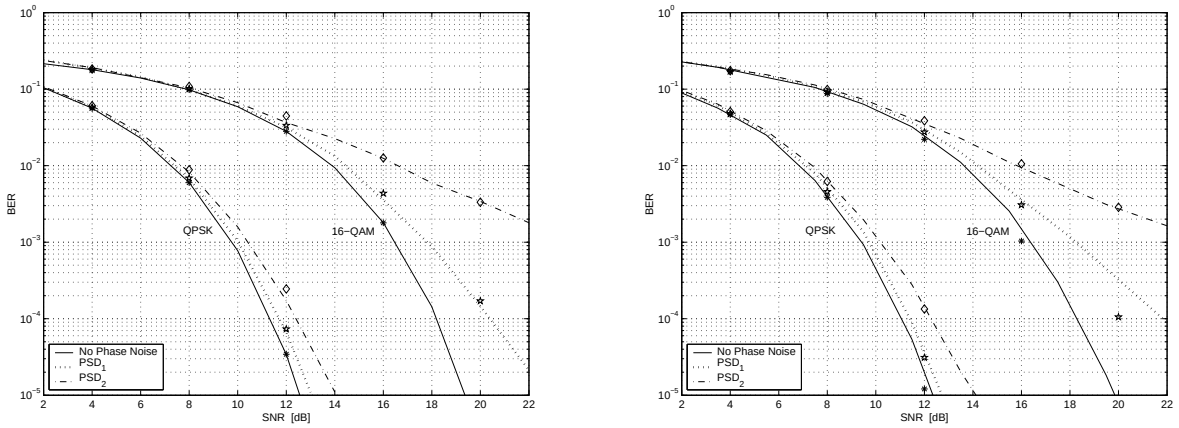

(a) DMT, $M = K = 128$ (b) NCS–FMT, $M = 128$, $K = 144$

Fig. 4. BER versus SNR for DMT and NCS–FMT in the presence of phase noise characterized by the PSDs given in Fig.2. The markers $\star, \diamond$, and $*$, indicate the theoretical bounds.

negligible with respect to the CPE and ISI contributions. Besides CPE, phase noise introduces a random component in the ISI which cannot be corrected by the equalizer (see (3)). This explains why the theoretical BER bounds that do not consider equalization practically match with the simulated equalizer performance. In this scenario, even tighter bounds could be obtained by extending to this context the method used for single–carrier modulation.

VIII. Conclusion

The effects of the phase noise in FMT modulated systems have been analyzed and compared to the DMT solution. Generally, phase noise introduces various interference components, i.e. common phase error, ISI and Intra/Inter-CI. The power of the interfering components has been evaluated, and its dependence on the phase noise spectra as well as the prototype filter shape has been demonstrated. The validity of the analytical results is confirmed by simulation results. Although Intra/Inter-CI is usually negligible for the commonly considered phase noise spectra, common phase error and ISI impact the FMT performance. Fast variations of the phase noise with respect to the length of the prototype filter increase the FMT bit/symbol error rate.

Appendix I
CPE, ISI and Intra/Inter–CI power evaluation

Let $f_{i,l}(nT)$ be the generic term that appears in (3)

$$f_{i,l}(nT) = \sum_{p=-\infty}^{+\infty} a_l(pT)\; z_{i,l}(pT, nT)\,.$$

$a_i(t)$ is a sequence of i.i.d. symbols, independent from $\vartheta(t)$. Then, the autocorrelation function of $f_{i,l}(t)$ reads:

$$\begin{aligned}\mathrm{r}_{f_{i,l}}(\tau) =& E\left[f_{i,l}(nT+\tau)\, f^*_{i,l}(nT)\right]\\ =& M_{a_i} \sum_{p=-\infty}^{+\infty} E\left[z_{i,l}(pT, nT+\tau)\, z^*_{i,l}(pT, nT)\right]\\ =& M_{a_i} \sum_{p=-\infty}^{+\infty} \mathrm{r}_{z_{i,l}}(pT,\tau) = M_{a_i}\, \mathrm{R}^{'}_{z}(f_1=0,\tau)\,,\end{aligned}$$

where the PSD $\mathrm{R}^{'}_{z}(f_1,\tau)$, $\tau \in \{-\infty, ..., -1, 0, 1, ..., +\infty\}$ is given by the Fourier transform of the correlation $\mathrm{r}_z(t_1,\tau)$ respect to t_1. Exploiting the PSD proprieties, the statistical power of $f_{i,l}(nT)$ is given by:

$$M_{f_{i,l}} = M_{a_i}\, \mathrm{R}^{'}_{z_{i,l}}(f_1=0,\tau=0) = M_{a_i} \int_{-\infty}^{+\infty} \mathrm{R}_{z_{i,l}}(0, f_2)\, df_2 \tag{23}$$

The argument of the integral in (23) reads $\mathrm{R}_{z_{i,l}}(f_1=0,f_2) = \mathrm{R}_{\vartheta_{i,l}}(f_2)\; |G_l(f_2)|^2\, |H_i(0)|^2$. Thus we obtain (10).

References

[1] G. Cherubini, E. Eleftheriou, and S. Ölçer "Filtered Multitone Modulation for Very High–Speed Digital Subscriber Lines", *IEEE JSAC*, vol.20, No.5, pp.1016–1028, June 2002.

[2] A. Assalini, S. Pupolin, and L. Tomba, "DMT and FMT Systems for Wireless Applications: Performance Comparison in the Presence of Frequency Offset and Phase Noise", *In. Proc. WPMC'03*, Yokosuka, Kanagawa, Japan, Oct. 2003.

[3] A. M. Tonello and A. Assalini, "An Asynchronous Multitone Multiuser Air Interface for High–Speed Uplink Communications", *In Proc. IEEE VTC'03 Fall*, Orlando, USA, Oct. 2003.

[4] A. Assalini and A. M. Tonello, "Time–Frequency Synchronization in Filtered Multitone Modulation Based Systems", *In. Proc. WPMC'03*, Yokosuka, Kanagawa, Japan, Oct. 2003.

[5] N. Benvenuto, G. Cherubini, and L. Tomba, "Achievable Bit Rates of DMT and FMT Systems in the Presence of Phase Noise and Multipath", in *Proc. IEEE VTC'00 Spring*, Tokyo, May 2000.

[6] A. Tonello, "Asynchronous Multicarrier Multiple Access: Optimal and Sub-optimal Detection and Decoding", *Bell Labs Technical Journal*, vol.7 No.3, pp.191-217, Feb. 2003.

[7] N. Benvenuto, S. Tomasin, and L. Tomba, "Equalization Methods in OFDM and FMT Systems for Broadband Wireless Communications", *IEEE Trans. on Comm.*, vol.50, pp.1413–1418, Sept. 2002.

[8] L. Piazzo and P. Mandarini, "Analysis of Phase Noise Effects in OFDM Modems", *IEEE Trans. on Comm.*, vol.50, pp.1696–1705, Oct. 2002.

[9] E. Costa and S. Pupolin, "M–QAM OFDM System Performance in the Presence of a Nonlinear Amplifier and Phase Noise", *IEEE Trans. on Comm.*, vol.50, No.3, pp.462–472, March 2002.

[10] P. Robertson and S. Kaiser, "Analysis of the Effects of Phase–Noise in Orthogonal Frequency Division Multiplex (OFDM) Systems", pp. 1652–1657 *In Proc. IEEE ICC'95*, Seattle, June 18–22, 1995.

[11] T. Pollet, M. Van Bladel, and M. Moeneclaey, "BER Sensitivity of OFDM Systems to Carrier Frequency Offset and Wiener Phase Noise", *IEEE Trans. on Comm.*, vol.43, pp.191–193, Feb./Mar./Apr. 1995.

[12] R. Corvaja and S. Pupolin, "Phase Noise Effects in QAM Systens", *In. Proc. PIMRC'97*, Helsinki, Finland, Sept. 1997.